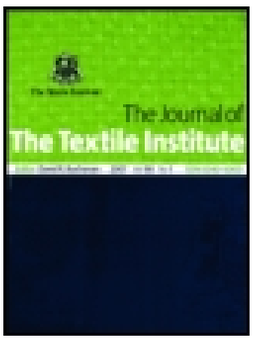

The Journal of The Textile Institute

ISSN: (Print) (Online) Journal homepage: https://www.tandfonline.com/loi/tjti20

Development and evaluation of pneumatic actuators for pediatric upper extremity rehabilitation devices

Bai Li, Huantian Cao, Ben Greenspan & Michele A. Lobo

To cite this article: Bai Li, Huantian Cao, Ben Greenspan & Michele A. Lobo (2021): Development and evaluation of pneumatic actuators for pediatric upper extremity rehabilitation devices, The Journal of The Textile Institute, DOI: 10.1080/00405000.2021.1929704

To link to this article: https://doi.org/10.1080/00405000.2021.1929704

Published online: 22 May 2021.

THE JOURNAL OF THE TEXTILE INSTITUTE
https://doi.org/10.1080/00405000.2021.1929704

Taylor & Francis
Taylor & Francis Group

RESEARCH ARTICLE

Development and evaluation of pneumatic actuators for pediatric upper extremity rehabilitation devices

Bai Li[a], Huantian Cao[b], Ben Greenspan[a] and Michele A. Lobo[a]

[a]Department of Physical Therapy & Biomechanics & Movement Science Program, University of Delaware, Newark, DE, USA; [b]Fashion & Apparel Studies Department, University of Delaware, Newark, DE, USA

ABSTRACT

Textile pneumatic actuators were developed to provide full assistance to lift the arm of a model of an 11-year-old male beyond 120 degrees of shoulder abduction. Two fabrics and a variety of sealing techniques, methods of attachment, and actuator shapes were comparatively evaluated using textile and functional tests. The results identified that both fabrics and one of the three sealing techniques were effective for creating air-tight, functional actuators. Actuators were more effective when the bands attaching them were closer to the axilla. Rectangular and wing-shaped actuators, both lifting the model of an 11-year-old male's arm above 120 degrees of abduction, were more effective than Y-shaped actuators. Multiple designs and materials may be acceptable for building textile pneumatic actuators to lift the full weight of a child's arm. Compared to traditional hard robots, soft assistive robots offer key potential benefits related to comfort, aesthetics, weight, bulk, and cost.

ARTICLE HISTORY
Received 16 June 2020
Accepted 10 May 2021

KEYWORDS
Soft actuators; exoskeleton; soft robot; rehabilitation technology; pediatrics

Introduction

Rehabilitation technology can increase independence for self-care activities, such as eating, grooming, and play, for children with upper extremity movement impairments due to arthrogryposis multiplex congenita, muscular dystrophy, spinal muscular atrophy, and other diagnoses (Babik et al., 2016; 2019; Estilow et al., 2018; Lobo & Li, 2021). There are a variety of devices, such as robotic exoskeletons and feeding devices, on the market to assist upper extremity function for people with physical disabilities. Exoskeletons are devices designed for wear that externally support the musculoskeletal system to enhance range of motion, reduce energy expenditure, assist weight-bearing, and improve functional performance of daily tasks (Exoskeleton Device – Mesh – NCBI, 2016; Veneman et al., 2006).

Although traditional exoskeletons can effectively assist limb movement, they are typically fabricated using metallic components, making them heavy, rigid, bulky, and uncomfortable for users (Li et al., 2019; Majidi, 2014; Realmuto & Sanger, 2019; Rus & Tolley, 2015). They are typically tethered (i.e. not portable) and expensive devices, which are difficult for users to access and utilize outside of laboratory or clinical environments (Babik et al., 2019; Realmuto & Sanger, 2019). The quickly evolving field of soft robotics has the unique potential to improve the portability, comfort, and aesthetics of exoskeletal devices (Nesler et al., 2018; Rus & Tolley, 2015). Soft robots are defined as systems "capable of autonomous behaviors and that are primarily composed of materials with moduli in the range of that of soft biological materials" (Rus & Tolley, 2015).

Actuators are devices that produce specific motions or actions when directed *via* input signals (Actuators, 2011). Pneumatic actuators are comprised of soft, air-proof materials and can provide substantial forces over relatively large areas (Li et al., 2019; Lobo et al., 2015; O'Neill et al., 2017; Simpson et al., 2017). In a few prior studies, pneumatic actuators have been developed as soft actuators to assist movement at the shoulder, with placement in different locations, such as near the axilla (Li et al., 2019; Lobo et al., 2015; O'Neill et al., 2017; Simpson et al., 2017), on the top of the upper limb (Natividad & Yeow, 2016), or around the upper limb (Natividad et al., 2018). There are two primary forms of pneumatic actuators: air muscles and inflatable bladders. Air muscles (e.g. McKibben artificial muscles) consist of an inner rubber cylinder layer constrained by an outer braided nylon layer. During inflation, the system functions such that its diameter increases and its length decreases, allowing it to "contract/shorten" like a muscle (Tsagarakis & Caldwell, 2003). An inflatable bladder or textile actuator is a fluid-impermeable bladder which contains a fluid-impermeable textile structure or a fluid-impermeable structure [e.g. a thermoplastic polyurethane (TPU) bladder] housed in the fabric pocket (Walsh et al., 2020). When actuated, the inflatable bladder can offer support to the body segment of the user.

Compared to most of the current exoskeletons that have rigid and bulky components, soft exoskeletons with pneumatic actuators have the potential to offer improved

CONTACT Michele A. Lobo malobo@udel.edu Department of Physical Therapy & Biomechanics & Movement Science Program, University of Delaware, 540 South College Ave., Room 210K, Newark, DE 19713, USA.

portability, comfort, and aesthetics. They can be made to feel soft, while being light weight, comfortable and affordable for users (Li et al., 2019; Manna & Dubey, 2018). Inflatable bladder actuators have the added potential of being sleek, as they can fold flat against the user's body when they are deflated, a benefit that may be appealing to users for discretion of the exoskeleton (O'Neill et al., 2017). There are several limitations in the existing research on soft exoskeletons. One limitation is the challenge of identifying a suitable method for inflation/deflation of the bladder. Battery-powered portable air compressors have been used but they create undesirable, high levels of noise (Simpson et al., 2017). Recently, portable compressed gas canisters have been applied as a solution with more promising results (Li et al., 2019; Simpson et al., 2017). Another limitation is that the existing research is limited in populations with disabilities, such as those with muscular weakness, who require greater support for their arms. Research with pneumatic exoskeletons has primarily focused on bench testing and preliminary testing with small numbers of healthy participants. Lastly, soft exoskeleton research could be enhanced by involving experts in textile science and apparel design who can conduct systematic evaluations to answer questions that have not yet been answered, such as which materials and methods are feasible and effective for fabricating soft exoskeletons.

The purpose of this study was to address the need for actuators that provide full arm support. The current research developed and comparatively evaluated soft pneumatic actuators made from sealed textile materials for future incorporation in a pediatric robotic device aimed at fully assisting shoulder abduction against gravity. The interdisciplinary team systematically evaluated the impact of textile characteristics, sealing technique, actuator shape, and method of attachment on functional performance of the actuator. We aimed to develop a textile pneumatic actuator to lift the full weight of the arm of a model of an 11-year-old boy into at least 120 degrees of shoulder abduction, a level sufficient for most functional upper extremity tasks.

Previous research has demonstrated that soft pneumatic bladders can be used to create a soft robotic limb that acts as an additional limb to support function (Nguyen et al., 2019). It has also shown that soft actuators comprised of plastic bladders housed in fabric casings can deliver partial assistance to reduce the muscle activity required to lift the arm for healthy adults (O'Neill et al., 2017; Simpson et al., 2017). Work from the corresponding author's group has demonstrated that actuators made from textiles can provide the full support, rather than just assistance, required to lift the arm of a model of an 11-year-old male (Li et al., 2019). Soft robotics work is in its early stages and there remains much to learn about how to optimally fabricate textile bladders, especially ones with the capacity to lift the full weight of the user's arm, a necessity when designing for individuals with more severe physical disabilities. The current study expands upon earlier work by systematically evaluating the functionality of textile pneumatic actuators fabricated to provide full support to pediatric users. Unlike earlier work, this research offers novel findings from textile testing, systematic evaluation of a variety of materials and fabrication methods, and a solution with the potential for do-it-yourself fabrication by community members. This novel textile and fabrication information is important to guide the development of improved soft exoskeletons. The do-it-yourself potential of the solution is important to increase the accessibility of the product for end users with physical disabilities (Hall & Lobo, 2018).

Materials and methods

Textile and functional testing were performed to identify the optimal sealing method for pneumatic actuator construction and to evaluate the functional performance of actuators varying in fabric properties, shapes, and method of attachment.

Textile characteristic

Two fabrics (Seattle Fabric, USA) with air proof coatings, making them heat sealable, were implemented in this study. They were: (1) 58″ Heat Sealable Coated Oxford (Oxford); and (2) 60″ Heat Sealable Coated Nylon Taffeta (Taffeta). The Oxford fabric count was 230 Ends Per Inch (EPI) and 180 Picks Per Inch (PPI). The Taffeta fabric count was 130 EPI and 115 PPI. The coating material for both the Oxford and Taffeta was TPU.

Textile testing was performed using the American Society for Testing and Materials (ASTM) International standards. Prior to testing, the samples were conditioned in an environmental chamber (Lunaire, Model No. CEO910-4, Thermal Product Solutions, New Columbia, PA, USA) at a temperature of 21 °C and relative humidity of 65% in accordance with ASTM D1776 (Standard Practice for Conditioning and Testing Textiles).

The fabric thickness was measured using a portable gauge (SDL Atlas Inc., Rock Hill, SC, Model: J100) and stiffness using a Handle-o-Meter (Thwing-Albert, West Berlin, NJ). The thickness was measured according to ASTM D1777-96 (2019) Standard Testing Methods for Thickness of Textile Materials. There were ten replications for each test. The stiffness was measured according to ASTM D1388-18 Standard Testing Method for Stiffness of Fabrics. There were five replications for each test.

Sealing method evaluation

To comparatively evaluate potential sealing methods for creating air-tight actuators, the researchers evaluated three sealing techniques. The actuators were sized to fit an 11-year-old male, with the length matching the measurement from waist to elbow. Six rectangular pneumatic actuators were created using the Oxford and Taffeta fabrics by sealing two 15.25 × 39.37 cm (6 × 15.5 inches) pieces of fabric using three sealing methods: 1) an impulse sealer (AIE-500, American INT'NL Electric); 2) a hand wheel sealer (ME-802HW, ABC Office); and 3) a flat iron (cs4wvd, CONAIR). The impulse sealer produced a 2 mm seal width using

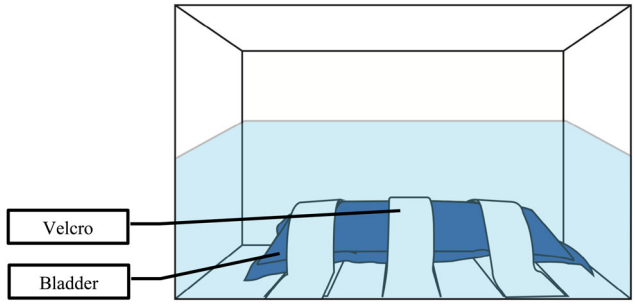

Figure 1. Volumetric measurement of the actuators, showing the three hook and loop straps holding the bladder at the bottom of the water bath.

temperatures between 190 and 205 °C; the hand wheel sealer produced a 5 mm seal width with an adjustable temperature range from 65 to 148 °C; and the flat iron produced a 19 mm seal width using temperatures up to 180.9 °C. The hand wheel sealer did not melt the coating on the air-proof fabrics, so this method was not a feasible sealing method. The researchers inflated the pneumatic actuators from the other two sealing methods and immersed them in a water bath.

Pressure was applied on each pneumatic actuator as shown in Figure 1 and visual observation was conducted (i.e. visual inspection for air bubbles in the water bath) to determine whether the seams were intact or allowed for air leakage. Leakage at the seams was observed for all of the pneumatic actuators created using the impulse sealer, while leakage was not observed for any of the pneumatic actuators constructed using the flat iron. Consequently, the flat iron method was used for sealing the fabrics for all of the following experiments. Temperature of the flat iron was measured by a Laser temperature gun (Lasergrip 774, Etekcity). The temperature was measured five times for each heat level; the results are shown in Table 1. The flat iron could reach a maximum of 180.92 °C and had twenty-five temperature options.

To determine the heat setting and duration associated with the strongest seal, the researchers used a Tinius Olsen (Horsham, PA, USA) HK5T benchtop tester and a modification of the ASTM D5034 Standard Test Method for Breaking Strength and Elongation of Textile Fabrics. The sealing method associated with the highest breaking strength would be most optimal for the fabrication of pneumatic actuators of high quality and durability. Fabric samples with the size of 7.62 × 20.32 cm (3 × 8 inches) were created by sealing two pieces of 7.62 × 11.43 cm (3 × 4.5 inches) fabric with a 1.27 cm (0.5 inch) seam line. The 8-inch length was in accordance with the ASTM D5034 standard method. The 3-inch width is shorter than the 4-inch sample width in the ASTM D5034 standard method. The reason to use the 3-inch width is that the length of the flat iron heating surface is 3 inches. Two sealing cycles would be required to seal a 4-inch length and the overlapping area might be sealed twice, which could affect the testing results.

Each fabric was tested in the warp and weft directions, evaluating the breaking strength of the seamline created *via* three different temperatures (levels 15, 20, and 25 on the flat iron) and three different heating durations (10, 30, and 60 s). Breaking strength was measured five times for each condition and descriptive results are reported (Table 2).

Table 1. Average temperatures [Mean (standard deviation)] of the flat iron settings tested.

Level	Off	15	20	25
Temperature (Unit: °C)	23.96 (.15)	140.08 (1.06)	155.78 (3.49)	180.92 (3.00)

To evaluate the effect of temperature (heat level) and duration (time) of heat sealing on the breaking strength of the seamline, two-way analysis of variance (ANOVA) was conducted separately across four fabric conditions: Oxford warp, Oxford weft, Taffeta warp, and Taffeta weft.

Actuator construction process

Three pneumatic actuators of each shape were fabricated by first creating paper patterns. The patterns were then traced on the Oxford and Taffeta fabrics. Two plastic barbed tube fitting valves (5463K594, McMaster-Carr) were then inserted into one of the pieces of fabric; both of the valves were placed in the midline of the pneumatic actuator. One valve was to connect to the air source and was placed 7.62 cm (3 inches) from the bottom of the pneumatic actuator (Figure 2). To connect the valve to the fabric, the researcher: (1) cut one small circular hole the size of the valve on one of the pneumatic actuator fabric pieces; (2) placed the valve in the circular holes, (3) secured the valves to the fabric using Super Glue (Gorilla Glue Company, 7805001-2), allowing the glue to fully dry; (4) applied hot glue around the circumference of the valve to secure it in place, ensuring the adhesive did not infiltrate the valve and block air flow and allowing the adhesive to fully dry; and (5) attached the silicone tubing to the outside opening of the valve. Once the valves had been placed, the two fabric pieces were sealed together using the parameters determined optimal from the earlier heat-sealing evaluation.

Functional testing

Three different actuator shapes were evaluated functionally with each fabric (Oxford and Taffeta). The shapes were a rectangle, wing, and Y shape (Figure 2). To characterize the size of the inflated actuators, the researchers evaluated their volume by inflating the actuators, immersing each actuator in a water bath, strapping it at the base, and recording the change in water level (as in Figure 1). This method also provided additional evidence that the seals were air-tight as no air was observed escaping from any of the actuators. Actuator volume (Table 3) after inflation is important because end users prefer exoskeletons to be as sleek as possible.

A 1-degree of freedom apparatus was constructed to simulate shoulder abduction (Figure 3). The weight of the arm matched that of an 11-year old male (2.70 kg). The length of the arm is 58.42 cm, and the weight is placed at the center of mass of the simulated arm. To evaluate the actuator using the testing apparatus, the researchers secured

Table 2. Results for the breaking strength testing [Mean (standard deviation)].

		Breaking strength (N)			
		Taffeta		Oxford	
Heating level	Heating time	Warp	Weft	Warp	Weft
15	10	35.06 (16.37)	18.83 (4.55)	13.00 (3.36)	16.86 (5.25)
	30	68.12 (16.68)	42.61 (30.80)	18.70 (2.65)	31.87 (8.99)
	60	57.84 (10.65)	56.94 (7.88)	34.37 (8.59)	33.94 (9.75)
20	10	146.36 (61.21)	177.55 (65.63)	125.23 (47.12)	115.96 (14.08)
	30	344.84 (98.70)	387.79 (82.72)	308.39 (22.94)	242.32 (63.24)
	60	461.04 (100.13)	436.71 (82.08)	403.72 (12.02)	380.26 (52.11)
25	10	528.20 (12.03)	507.25 (29.62)	381.96 (23.06)	338.72 (36.32)
	30	533.80 (38.43)	529.20 (29.46)	365.12 (7.08)	340.24 (18.09)
	60	645.60 (23.63)	569.65 (82.21)	383.91 (25.31)	393.32 (18.50)

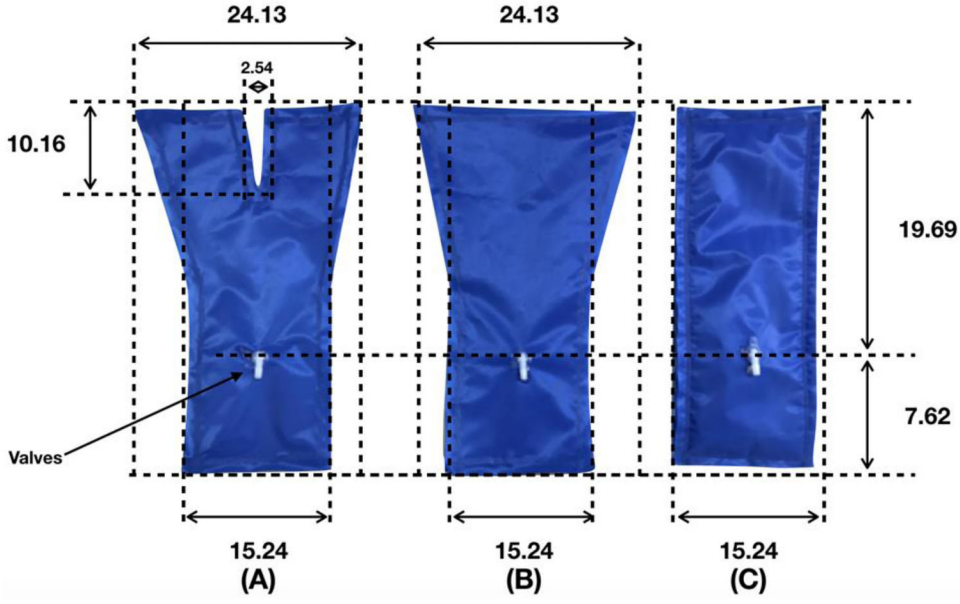

Figure 2. The actuator shapes tested: (A) Y, (B) Wing, (C) Rectangular shape (unit of measure is cm). A valve to allow for bladder inflation can be seen on each actuator.

Table 3. Maximum actuator volume, shoulder abduction angle achieved, and air pressure in the actuator for each fabric and shape [Mean (standard deviation)].

	Coated Oxford			Nylon Taffeta		
	Rectangular-shaped	Wing-shaped	Y-shaped	Rectangular-shaped	Wing-shaped	Y-shaped
Volume (cm^3)	1963.99 (189.94)	2509.51 (189.94)	1527.44 (189.94)	2291.24 (189.94)	2662.24 (113.40)	2072.96 (327.41)
Angle (degrees)	148.28 (1.94)	142.09 (2.42)	120.04 (2.56)	149.08 (0.18)	145.64 (4.23)	113.2 (0.86)
Pressure (PSI)	4.95 (0.1)	6.32 (1.26)	5.45 (0.22)	5.06 (0.01)	4.99 (0.23)	5.28 (0.06)

each actuator in the axilla of the testing apparatus using 5.08 cm wide heavy-duty hook and loop fasteners (Velcro) and 5.08 cm wide elastic belts (iCraft; Figure 3). The actuator was inflated to achieve its maximum shoulder abduction angle across three consecutive trials using an air compressor (Hitachi EC28M).

Air pressure within the pneumatic actuator was recorded continuously using a pressure sensor (Adafruit MPRLS Ported Pressure Sensor). Two instruments, that is, a commercial motion capture system (TrakSTAR, Ascension Technology Corporation) and a 3-axis accelerometer (ADXL335, Adafruit Industries), were used to simultaneously measure the maximum shoulder abduction angle. The TrakStar motion capture system has been used in several published robotics studies (Field et al., 2011; Polygerinos et al., 2015; Song et al., 2015; Tausch et al., 2012); and using accelerometers to measure movement read through an Arduino is becoming increasingly common. To validate the accelerometer sensor for measuring maximum shoulder abduction angle, the researchers conducted a paired sample t-test to assess the difference between the data collected with the accelerometer sensor and the TrakStar sensor.

To evaluate the placement of the elastic bands attaching the bladder to the model, this functional testing protocol was performed with both belts as close to the model's joint (0 cm) as possible or with each belt 7.62 cm from the joint in each direction. Testing was repeated with rectangular

pneumatic actuators made with the Oxford and Taffeta fabrics. To analyze the effect of the two fabric types and two attachment methods on the maximum abduction angle, a two-way ANOVA was conducted.

To evaluate the impact of the fabric type and actuator shape on functional performance, six pneumatic actuators, one rectangular, one wing, and one Y-shaped pneumatic actuator in each fabric type (Oxford and Taffeta), were fabricated and tested using the functional testing protocol. A two-way ANOVA was conducted to analyze the results.

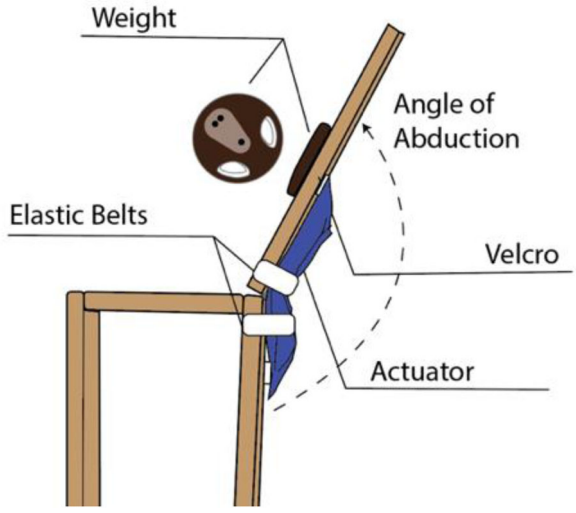

Figure 3. The functional testing apparatus allowing for abduction movement at the shoulder and weighted to match the arm of an 11-year-old male. The pneumatic actuator is attached under the model's axilla by securing it to hook and loop fabric and then encompassing it with elastic belts.

Results

Fabric thickness and stiffness

The Taffeta fabric was thinner and less stiff than the Oxford fabric. The thickness of the Oxford fabric was .263 mm (S.D. = .003), and the thickness of the Taffeta fabric was .177 mm (S.D. = .002). The stiffness of the Oxford fabric was greater than 100 g (out of the test range of 100 g) and the stiffness of the Taffeta fabric was 47.915 g (S.D. = 2.508).

Sealing method evaluation

When the Oxford fabric was sealed in the warp or the weft direction, there was a statistically significant interaction between the effects of heat level and duration of heating on the seamline breaking strength [warp: $F(4, 36) = 10.877$, $p < .01$; weft: $F(4, 36) = 20.381$, $p < .01$]. As shown in Figure 4A and B, the breaking strength of seamlines generated with the flat iron at level 25 was the highest across all of the durations of heating for both the warp and weft directions.

When the Taffeta fabric was sealed in the warp or weft direction, there was a statistically significant interaction between the effects of heat level and duration of heating on

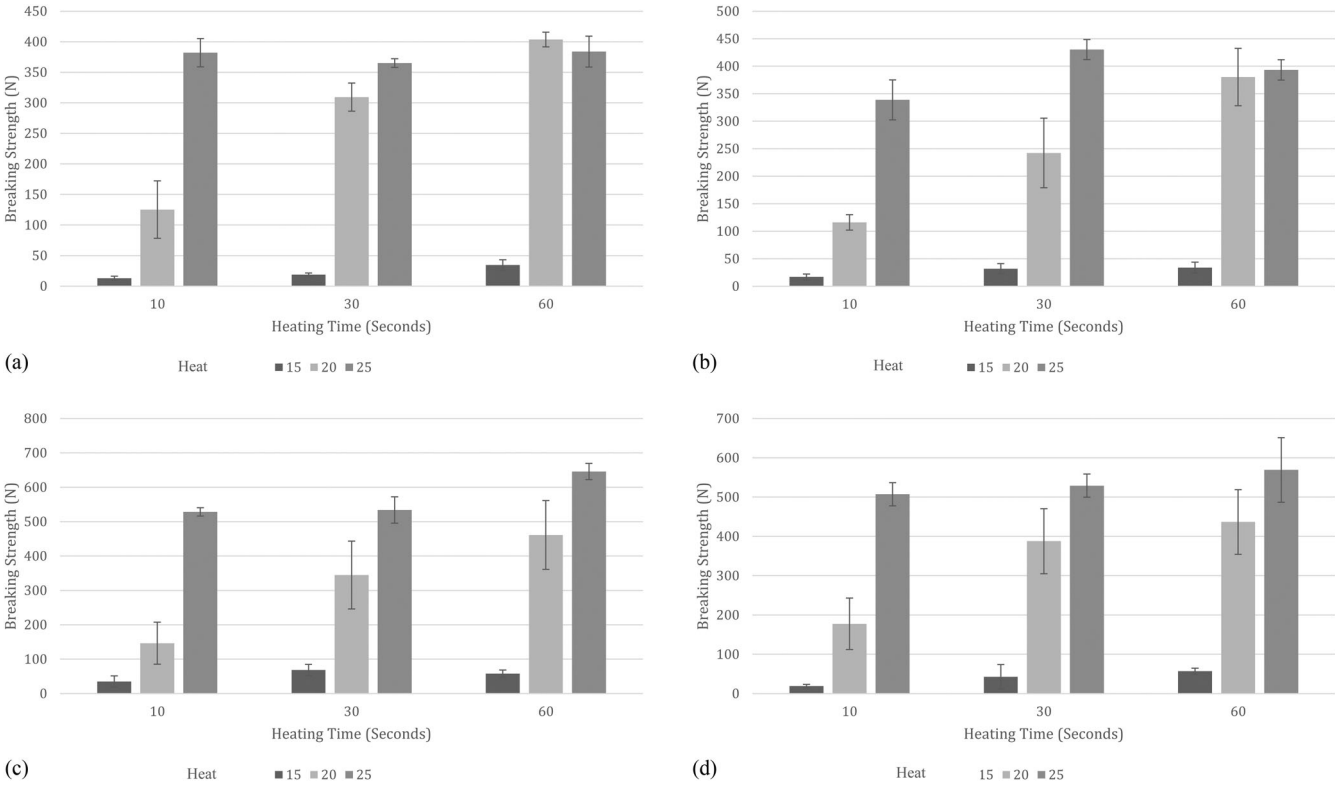

Figure 4. (A) The estimated marginal means of breaking strength for the Oxford fabric sealed with the flat iron in the warp direction (error bars represent standard deviation); (B) The estimated marginal means of breaking strength for the Oxford fabric sealed with the flat iron in the weft direction (error bars represent standard deviation); (C) The estimated marginal means of breaking strength for the Taffeta fabric sealed in the warp direction (error bars represent standard deviation); and (D) The estimated marginal means of breaking strength for the Taffeta fabric sealed in the weft direction (error bars represent standard deviation).

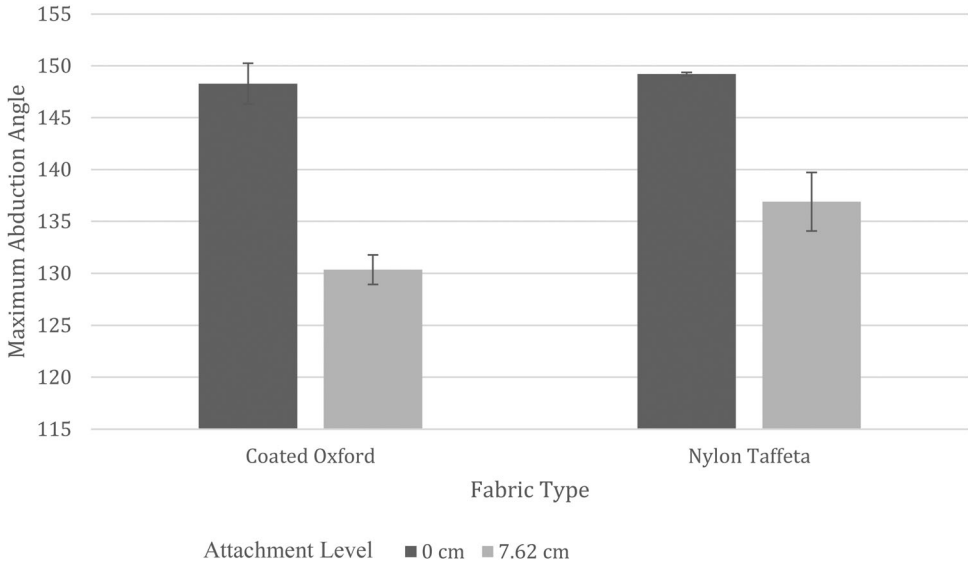

Figure 5. Maximum shoulder abduction angles reached during functional testing comparing the two different locations for the elastic belts attaching the Oxford and Taffeta pneumatic actuators (error bars represent standard deviation).

the seamline breaking strength [warp: F (4, 36) = 20.381, $p < .01$; weft: F (4, 36) = 22.366, $p < .01$). As shown in Figure 4C and D the breaking strength of seamlines generated with the flat iron at level 25 was the highest for the 10- and 30-second durations of heating. The breaking strength of seamlines generated with the flat iron at levels 20 and 25 were higher than that generated by level 15 for the 60-second duration of heating for both conditions.

These results suggested that strong seamlines could be obtained with both fabrics, although the Oxford produced stronger results ($p < .01$; breaking strength for the Oxford fabric: $M = 303.85$ N, S.D. = 220.87, Taffeta: $M = 219.42$ N, S.D. = 162.06). They also suggested fabric direction should be considered when fabricating pneumatic actuators as seamlines along the warp direction were stronger ($p < .000$; breaking strength in the warp direction: $M = 270.94$ N, S.D. = 207.31, weft direction: $M = 252.33$ N, S.D. = 188.42).

Furthermore, using the flat iron at heat level 25 (180.92 °C) for 10 s could produce strong seams while allowing for greater efficiency in fabrication. These heat-sealing parameters were used to create the soft actuators for the remainder of the functional testing.

Functional testing

There was no significant difference in the maximum shoulder abduction angle measured by the accelerometer or the TrakSTAR system, t (53) = .286, $p = .776$, supporting the accuracy of the accelerometer sensor data. Accelerometer sensor data are presented throughout the results below since they were accurate while offering the benefit of ease of synchronization with the accelerometer pressure sensor data.

Functional testing results are shown in Figure 5. There was no significant interaction between the fabric type and attachment method (F (1, 8) = 7.141, $p = .028$). There was no difference in maximum abduction angle in relation to fabric type ($p = .502$). There was a difference in maximum abduction angle in relation to method of attachment.

The findings suggest that both fabrics can be used to create functional pneumatic actuators. In addition, both integration methods can result in shoulder abduction angles greater than 120 degrees. However, greater angles of abduction can be achieved when bands are placed at the axilla. It should be noted that while band placement at the axilla can lead to greater abduction angles on the model, it may be a challenging method to implement on human participants depending on the amount of compression it places on the axilla, an area that houses nerves and blood vessels that should not be constricted.

There was no significant interaction between the fabric type and shape on the maximum abduction angle, [F (2, 30) = .310, $p = .736$; Table 3]. There was no significant difference in function (shoulder abduction angle) between the two fabric types ($p = .673$). However, as shown in Table 3, the maximum shoulder abduction angle obtained was greater for the rectangular pneumatic actuators ($M = 148.68°$, S.D. = 1.32), and the wing-shaped pneumatic actuators ($M = 145.63°$, $S.D = 4.23$.) than the Y-shaped pneumatic actuators ($M = 116.62°$, S.D. = 4.12).

These results suggest the rectangular and wing-shaped actuators made using either the Oxford or Taffeta were effective at reaching shoulder abduction angles greater than 120°. As shown in Table 3, the maximum air pressure readings within the pneumatic actuators during the functional testing were at levels that would be safe for human wear (4.95 ± .1 to 6.32 ± 1.26 psi) (Guiochet et al., 2003)

Discussion

Both fabrics evaluated could be used to create functional actuators. However, only one of the three sealing tools tested, heating with a flat iron (cs4wvd, CONAIR), could successfully be used to create air-tight seams with the fabrics. In thermal bonding of textiles, softened or melted adhesive enters the irregular and porous textile surface to provide mechanical interlocking, thus temperature, pressure,

and pressing time are important parameters to determine the bonding strength (Jakubčionienė & Masteikaite, 2010). Using TPU as an adhesive to bond textiles, Jakubčionienė and Masteikaite (2010) found that 180 °C was the optimal temperature, while Daukantienė et al. (2021) found that 150 °C was the optimal temperature associated with the highest bonding strength. Compared to research that kept pressing time constant, e.g. 20 s (Daukantienė et al., 2021) or 30 s (Jakubčionienė & Masteikaite, 2010), and only changed temperature, this research tested both temperature and pressing time and verified that there existed a significant interaction effect between temperature and pressing time on the bonding strength. It was identified that the optimal heat setting and duration of heating with the flat iron to maximize the breaking strength of the seam were Level 25 (180.92 °C) and 10 s. Using a short sealing time of 10 s could minimize fabrication time.

Implementation of fabric bands to attach the actuator enabled greater shoulder abduction angles when placed at the axilla rather than more distal to the joint. However, user comfort and integrity of the nerves and blood vessels in the axilla will need to be considered when translating this solution into practice with human participants. Rectangular and wing-shaped actuators raised the model arm to the highest levels of shoulder abduction, while Y-shaped actuators fell at or just below the target of 120 degrees of shoulder abduction. Air pressure in all of the pneumatic actuators remained within safe ranges.

Prior to this study, the research team created the preliminary design of a soft pneumatic exoskeleton that could lift a human 11-year-old child's arm greater than 90 degrees (Li et al., 2019). The current study extended this work by systematically evaluating the methods involved in actuator design in order to create an actuator that could lift the arm more effectively. The result was the identification of materials and techniques that can be used to create actuators that successfully lift a model arm with the weight of an 11-year-old male to more than 120 degrees of shoulder abduction. Future directions for this research are to test the actuators on a model with more than one degree of shoulder motion, to integrate the actuators within garments that can be worn, and to test the soft exoskeleton on children with upper limb movement disabilities, assessing its usability and function.

This study provides evidence that a variety of fabrics and designs may be used to develop functional pneumatic actuators. Those alternatives can provide users a greater number of options for solutions to best match their comfort and aesthetic needs. The results of this study serve as a reference to guide future studies involving soft actuator fabrication and integration processes. Compared to traditional robotic exoskeletons, soft designs have the potential to be more comfortable, affordable, and aesthetically appealing (Li et al., 2019; Majidi, 2014; Rus & Tolley, 2015). The potential use for this design is not limited to children with disabilities; it may also be helpful in assisting geriatric populations or for performance enhancement and energy savings in healthy adults (Kim et al., 2019; O'Neill et al., 2017; Simpson et al., 2017).

Conclusion

This study has demonstrated that soft, pneumatic actuators made entirely of fabric can provide the full level of assistance necessary to successfully raise the arm of a model simulating the weight of an 11-year-old male to greater than 120 degrees of shoulder abduction. In addition, this study indicated that the textile properties, actuators shapes, and method of attachment, are crucial factors for the functional performance of the actuator.

Acknowledgements

The researchers would like to thank the parents and children who have shared information regarding their needs for this type of device, those participating in testing of prototypes, and research assistants helping with this project.

Disclosure statement

No potential conflict of interest was reported by the authors.

Funding

Supported by the National Science Foundation (1722596, Lobo), and a UNIDEL supported Henswear Pilot Project Grant (Lobo and Cao).

References

Actuators. (2011). *Science direct*. Retrieved June 12, 2020, from https://www.sciencedirect.com/topics/engineering/actuators

Babik, I., Cunha, A. B., & Lobo, M. A. (2019). Play with objects in children with arthrogryposis: Effects of intervention with the Playskin Lift™ exoskeletal garment. *American Journal of Medical Genetics Part C: Seminars in Medical Genetics*, 181(3), 393–403. https://doi.org/10.1002/ajmg.c.31719

Babik, I., Kokkoni, E., Cunha, A. B., Galloway, J. C., Rahman, T., & Lobo, M. A. (2016). Feasibility and effectiveness of a novel exoskeleton for an infant with arm movement impairments. *Pediatric Physical Therapy*, *28*(3), 338–346. https://doi.org/10.1097/PEP.0000000000000271

Daukantienė, V., Danilovas, P. P., & Mikalauskaitė, G. (2021). Study of temperature impact on the behaviour of fiber polymer materials' and their adhesive bond. *The Journal of the Textile Institute*, *112*(2), 313–321. https://doi.org/10.1080/00405000.2020.1746011

Estilow, T., Glanzman, A. M., Powers, K., Moll, A., Flickinger, J., Medne, L., Tennekoon, G., & Yum, S. W. (2018). Use of the Wilmington robotic exoskeleton to improve upper extremity function in patients with Duchenne muscular dystrophy. *American Journal of Occupational Therapy*, *72*(2), 7202345010p1–7202345010p5. https://doi.org/10.5014/ajot.2018.022939

Exoskeleton Device – Mesh – NCBI. (2016). Retrieved February 19, 2021, from https://www.ncbi.nlm.nih.gov/mesh/?term=exoskeleton%2Bdevices

Field, M., Pan, Z., Stirling, D., & Naghdy, F. (2011). Human motion capture sensors and analysis in robotics. *Industrial Robot: An International Journal*, *38*(2), 163–171. https://doi.org/10.1108/01439911111106372

Guiochet, J., Tondu, B., Baron, C. (2003). Integration of UML in human factors analysis for safety of a medical robot for tele-echography. *Proceedings 2003 IEEE/RSJ International Conference on Intelligent Robots and Systems (IROS 2003)* (Cat. No. 03CH37453), Vol. 4, pp. 3212–3217. IEEE.

Hall, M. L., & Lobo, M. A. (2018). Design and development of the first exoskeletal garment to enhance arm mobility for children with

movement impairments. *Assistive Technology*, *30*(5), 251–258. https://doi.org/10.1080/10400435.2017.1320690

Jakubčionienė, Ž., & Masteikaite, V. (2010). Investigation of textile bonded seams. *Materials Science*, *16*(1), 76–79.

Kim, J., Lee, G., Heimgartner, R., Arumukhom Revi, D., Karavas, N., Nathanson, D., Galiana, I., Eckert-Erdheim, A., Murphy, P., Perry, D., Menard, N., Choe, D. K., Malcolm, P., & Walsh, C. J. (2019). Reducing the metabolic rate of walking and running with a versatile, portable exosuit. *Science*, *365*(6454), 668–672. https://doi.org/10.1126/science.aav7536

Li, B., Greenspan, B., Mascitelli, T., Raccuglia, M., Denner, K., Duda, R., & Lobo, M. A. (2019, April). *Design of the playskin Air^{TM}: A user-controlled, soft pneumatic exoskeleton* [Paper presentation]. *2019 Design of Medical Devices Conference*, American Society of Mechanical Engineers Digital Collection, Minneapolis, MN. April 15–18, 2019. V001T03A004. ASME. https://doi.org/10.1115/DMD2019-3231

Lobo, M. A., & Li, B. (2021, October). Feasibility and effectiveness of a soft exoskeleton for pediatric rehabilitation. *The International Symposium on Wearable Robotics (WeRob2020) AND Wearracon Europe*. Spring, Cham. https://www.springer.com/gp/book/978303069

Lobo, J., Doyle, J., Thompson, C., Szczepanek, G., & Marcozzi, A. (2015, April 13-16). Playskin Air^{TM}: Pediatric exoskeletal garment. *2015 Design of Medical Devices Conference – International Student Design Showcase*.

Majidi, C. (2014). Soft robotics: A perspective—current trends and prospects for the future. *Soft Robotics*, *1*(1), 5–11. https://doi.org/10.1089/soro.2013.0001

Manna, S. K., & Dubey, V. N. (2018). *Design proposal for a portable elbow exoskeleton* [Paper presentation]. 2018 Design of Medical Devices Conference, American Society of Mechanical Engineers Digital Collection, Minneapolis, MN, April 9–12, 2018. V001T03A013. ASME. https://doi.org/10.1115/DMD2018-6931

Natividad, R. F., Hong, S. W., Miller-Jackson, T. M., & Yeow, C. H. (2018).The exosleeve: A soft robotic exoskeleton for assisting in activities of daily living. In Biosystems & Biorobotics (pp. 406–409). https://doi.org/10.1007/978-3-030-01887-0_78

Natividad, R. F., & Yeow, C. H. (2016, June). *Development of a soft robotic shoulder assistive device for shoulder abduction* [Paper presentation]. 2016 6th IEEE International Conference on Biomedical Robotics and Biomechatronics (BioRob) (pp. 989–993). IEEE. https://doi.org/10.1109/BIOROB.2016.7523758

Nesler, C. R., Swift, T. A., & Rouse, E. J. (2018). Initial design and experimental evaluation of a pneumatic interference actuator. *Soft Robotics*, *5*(2), 138–148. https://doi.org/10.1089/soro.2017.0004

Nguyen, P. H., Mohd, I. I., Sparks, C., Arellano, F. L., Zhang, W., & Polygerinos, P. (2019). *Fabric soft poly-limbs for physical assistance of daily living tasks* [Paper presentation]. 2019 International Conference on Robotics and Automation (ICRA). (pp. 8429–8435). IEEE. https://doi.org/10.1109/ICRA.2019.8794294

O'Neill, C. T., Phipps, N. S., Cappello, L., Paganoni, S., & Walsh, C. J. (2017). *A soft wearable robot for the shoulder: Design, characterization, and preliminary testing* [Paper presentation]. 2017 International Conference on Rehabilitation Robotics (ICORR), July (pp. 1672–1678). IEEE.

Polygerinos, P., Wang, Z., Galloway, K. C., Wood, R. J., & Walsh, C. J. (2015). Soft robotic glove for combined assistance and at-home rehabilitation. *Robotics and Autonomous Systems*, *73*, 135–143. https://doi.org/10.1016/j.robot.2014.08.014

Realmuto, J., & Sanger, T. (2019). *A robotic forearm orthosis using soft fabric-based helical actuators* [Paper presentation]. 2019 2nd IEEE International Conference on Soft Robotics (RoboSoft) (pp. 591–596). IEEE. https://doi.org/10.1109/ROBOSOFT.2019.8722759

Rus, D., & Tolley, M. T. (2015). Design, fabrication and control of soft robots. *Nature*, *521*(7553), 467–475. https://doi.org/10.1038/nature14543

Simpson, C. S., Okamura, A. M., & Hawkes, E. W. (2017). *Exomuscle: An inflatable device for shoulder abduction support* [Paper presentation]. 2017 IEEE International Conference on Robotics and Automation (ICRA) (pp. 6651–6657). IEEE. https://doi.org/10.1109/ICRA.2017.7989785

Song, S., Li, Z., Meng, M. Q. H., Yu, H., & Ren, H. (2015). Real-time shape estimation for wire-driven flexible robots with multiple bending sections based on quadratic Bézier curves. *IEEE Sensors Journal*, *15*(11), 6326–6334. https://doi.org/10.1109/JSEN.2015.2456181

Tausch, T. J., Kowalewski, T. M., White, L. W., McDonough, P. S., Brand, T. C., & Lendvay, T. S. (2012). Content and construct validation of a robotic surgery curriculum using an electromagnetic instrument tracker. *Journal of Urology*, *188*(3), 919–923. https://doi.org/10.1016/j.juro.2012.05.005

Tsagarakis, N. G., & Caldwell, D. G. (2003). Development and control of a 'soft-actuated' exoskeleton for use in physiotherapy and training. *Autonomous Robots*, *15*(1), 21–33. https://doi.org/10.1023/A:1024484615192

Veneman, J. F., Ekkelenkamp, R., Kruidhof, R., van der Helm, F. C., & van der Kooij, H. (2006). A series elastic-and bowden-cable-based actuation system for use as torque actuator in exoskeleton-type robots. *The International Journal of Robotics Research*, *25*(3), 261–281. https://doi.org/10.1177/0278364906063829

Walsh, C. J., O'Neill, C. T., & Phipps, N. S. (2020). Textile Actuators. US20200170873A1.